

## Effect of rice husk ash addition on the physical properties of soda-lime-silica glass for building glass and window panel

M.F.F.S Alazemi<sup>1</sup>, M.N Abdullah<sup>2</sup>, F. Mustapha<sup>2</sup>, M.K.A Ariffin<sup>1</sup>, E.E Supeni<sup>1</sup>

<sup>1</sup> Department of Mechanical and Manufacturing Engineering, Faculty of Engineering, Universiti Putra Malaysia, 43400 UPM, Malaysia

<sup>2</sup> Department of Aerospace Engineering, Faculty of Engineering, Universiti Putra Malaysia, 43400 UPM, Malaysia

**ABSTRACT** – Demand for eco-friendly materials are increasing each year due to their excellent properties, which has proved to contribute in developing sustainable environment. One of the promising raw materials in producing glass is rice husk, a waste product from paddy harvesting, which contains about 90% of silica. Rice husks are usually burnt in an open area and contributed to serious air pollution problems. In this research, Soda-Lime-Silica Rice Husk Ash (SLRHA) glass which is a new combination of soda lime silicate (SLS) glass and rice husk ash (RHA) was developed for building glass and window application. The physical properties of the developed SLS-RHA glass system is presented in this paper. Based on the ultrasonic velocities test, sample with 5% of RHA was found to possess high and medium elastic properties including easy to bend rather than elongate, less stiff, tough at a certain direction and has low rigidity. Sample with 0% and 10% of RHA showed medium and poor elastic properties, respectively. High hardness value of the RHA glass was achieved using combinations of 60 to 120 Rockwell hardness test scale with up to 2% RHA. By considering the results from both tests, sample with 0% to 5% of RHA was considered to be the optimum formulation in the production of building glass and window panel.

### ARTICLE HISTORY

Received: 21<sup>st</sup> Sept 2019

Revised: 30<sup>th</sup> Sept 2020

Accepted: 4<sup>th</sup> Dec 2020

### KEYWORDS

*Rice husk ash;*  
*Soda Lime Silica glass;*  
*elastic properties;*  
*microstructural analysis;*  
*mechanical properties*

## INTRODUCTION

Eco-friendly materials can be described as a product that sustainable without harmful to the environment [1]. Rice husk can be one of capable eco-friendly material where waste product from paddy plant [2]. Eco-friendly product may seem to be more expensive, but for the long-term sustainable, the eco-friendly material more efficient in term of cost for the long term [3]. The conventional material has their own short life cycle and it is significant subject to materials limitations, chemical recovery, and biodegradability compared to the eco-friendly that has the capability of recycling. When harvesting paddy, rice husk (RH) which is the very outer layer is the main residues during the rice milling process. Incineration of RH resulted in rice husk ash (RHA). This has stimulated a great deal of research interests because of its high silica content as well as the abundant availability of RH, the starting material, at low cost. Several researchers who are using RHA as a source material for their investigations are necessarily to determine the chemical composition of the RHA used in their study. Generally, RHA should be contained around 87 to 97% amorphous silica and some trivial amounts of alkalis and other remnant components. Dissimilar of RHA constituents are due to geological influences, locations soil chemistry, yielding year, analyses approach and experiment preparation [4].

Agricultural waste product including rice husk has huge potential to be a new alternative to the conventional material used for building glass and window panel. RH was obtained from paddy milling process. Many countries take the easiest way to dispose of the RH by burnt it in open area. The burning of rice husk will give the environmental impact to the earth [5]. According to the statistic, the global production of paddy will reach around 650 million tons in 2050 [6]. It also reported that every ton of rice will produce around 0.23 tons of RH. In general, paddy consists of 72% of rice, 20% to 22% of husk, and another 5% to 8% of bran. To get the high purity of silica, RH needs to undergo some heat treatment. Mainly, the treatment of the rice husk will give approximately 90% of silica in the form of crystalline structure [7]. Crystalline of RHA becoming the most wanted materials in the production ceramics, steel industries and for the production of refractory bricks due to refractory properties in the RHA [8].

SLS glass, also called soda-lime-glass, is the most common type of glass used for windowpanes, glass containers and flat glass [9]. Most commercially made glasses are composed primarily of silica (70.980 wt %). In addition to silica, glasses also contain other oxides such as CaO, Na<sub>2</sub>O, K<sub>2</sub>O and Al<sub>2</sub>O<sub>3</sub>, which influence their properties [10]. Sintering phenomenon also affects the SLS glass structure. Prado et al. [11] found that as a result of sintering at temperature above 680°C, the glass will develop a crystalline structure and increases the density of SLS glass and decreases its apparent porosity.

The objective of this research is to develop an optimum formulation for an eco-friendly RHA-based material for the production of building glass and window panel. Commercial SLS glass was added to RHA to take advantage of SLS glass's chemical stability to improve the resistance of the glass to cracking. Study on the microstructure properties of RH after leaching and heat treated at 600°C for two hours, was conducted to investigate the behavior of the rice husks. RH

glass samples are then test for Rockwell hardness and ultrasonic wave velocity tests. From the tests, the suitability of RHA-based material as building glass and window was identified.

## METHODS AND MATERIALS

### Preparation of Rice Husk Ash

RH was supplied by Bernas rice milling factory in Tanjung Karang, Selangor, Malaysia and contains almost 75 to 90% of organic materials such as cellulose, lignin, and hemicellulose [9]. RH was pre-treated with distilled water and leached with 1 M HCL solution in the standard room temperature to remove the other impurities material and dirt in the rice husk. The optimum ratio for HCL was 100 mL and was poured into a beaker with an amount of 10 grams RH. Hei-Standard Magnetic stirrer in UPM Chemical Engineering Lab was used to heat the beaker. Once the temperature reached 60°C, vigorous stirring of the mixture started for 30 minutes continuously along the process. Thermometer was constantly put into the beaker to ensure the 60°C temperature was throughout of the mixture. Unwanted HCL was required to be discarded carefully as it could be corrosive to others. The RHA was filtered using a standard stainless-steel mesh screen and washed completely with distilled water to remove any remaining HCL solution and solid residue. RH was then dried in an oven for 2 hours at 110°C. This process was to ensure the RH were being completely dried before the incineration step. WiseTherm Digital Muffle Furnace was used for incinerating dried RH into RHA with controlled temperature of 600 for two hours. The RHA produced are then grinded into fine particles size using pulverizing machine RT-02A and sieved using Endecotts Laboratory Test Sieve 75  $\mu\text{m}$  to obtain an average particle size below 75  $\mu\text{m}$ . RHA particle is shown in Figure 1.



**Figure 1.** RHA particle: (a) before ground and sieved and (b) after ground and sieved

### Preparation of Soda Lime Silica-Rice Husk Ash Glass

The materials needed for fabricating the glass is soda-lime silicate (SLS) glass powder and rice husk ash (RHA). To produce SLS glass powder, the waste SLS glass bottle was crushed using mortar and pestle until the glass powder ground to the size of smaller than 200  $\mu\text{m}$ . The SLS glass powder are then mixed together with different ratio of RHA. Samples of RHA glass with three duplication were prepared using a melt quenching technique. The ratio of the RHA is 0%, 5%, and 10% from the total mass sample. The total mass of the mixture is 30.0 g that will place into the glass mould after the heating process. The total sample powder weight for each series is 30.0 g. The composition of the glasses investigated is given in Table 1.

**Table 1.** The compositions of SLS-RHA glass ratio.

Sample	RHA weight (g)	SLS weight (g)	Sample powder weight (g)
1	0	30.0	30.0
2	1.5	28.5	30.0
3	3.0	27.0	30.0

The SLS powder and RHA were mixed using dry milling machine to obtain a homogenous sample powder. The process of milling was continued for 2 hours and repeated for another sample with different compositions. After the milling process was done, the sample powder was transferred to an alumina crucible. To reduce the tendency to volatilization, the crucible containing the sample mixture powder was required to be preheated at 450°C for a period of one hour. After the preheating process, the crucible was transferred into electric furnace for melting process at 1400°C

for two hours. This process is to ensure the sample powder melt homogeneously. For the casting process, stainless-steel plate was used as a mould for glass melting process. The stainless-steel mould needs to be preheated at 450°C for 30 min. The melting glass in the crucible was taken out from the electric furnace and poured into the stainless steel mould. Then, annealing process is required to stabilize the glass structure. Samples are annealed in an electric furnace for 1 hour at 450°C. After the annealing process was done, the glass samples were allowed to cool down at room temperature. The overall process of the preparation of SLS-RHA glass is shown in Figure 2.

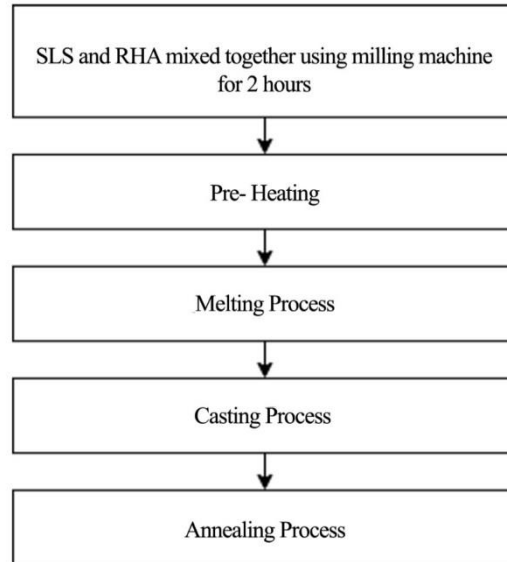


**Figure 2.** Glass fabrication process

### Preparation of SLS-RHA Glass Sample

SLS-RHA glass samples were cut to a dimension of 1.0 cm × 1.0 cm × 0.1 cm using Buehler Isomet low speed saw machine. Low speed saw machine was used to avoid cracking on the glass samples. A smooth surfaces on each side of the glass surface is important to obtain accurate data in optical properties test. In order to reduce the friction between glass samples and diamond cutter, lubricant oil was used during the cutting process. Finally, silicon carbide paper was used to polish these glass samples to remove cutting deformation marks and for better smooth surface of glass samples before further analysis. Glass samples after polished is shown in Figure 3.

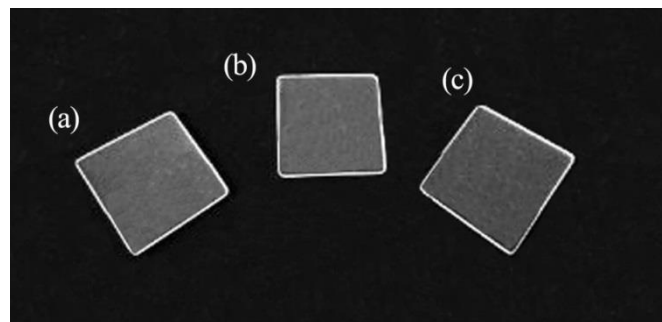


**Figure 3.** SLS-RHA glass samples: (a) 0% wt. RHA, (b) 5% wt. RHA and (c) 10% wt. RHA

### Ultrasonic Wave Velocity Test

The ultrasonic test was conducted using MATEC Model MBS8000 DSP (ultrasonic digital signal processing) system which is using the pulse-echo technique. The goal for this test is to determine the elastic properties of RHA glass using the value of the ultrasonic wave velocity, value of longitudinal and shear time internal obtained from the ultrasonic test machine. Based on the output result which is the ultrasonic wave velocity of longitudinal and shear, can be determined. The ultrasonic wave velocity can be calculated using Equation 1, where  $X$  is the sample thickness were all the glass samples have the same thickness, which is 10mm.  $\Delta t$  is the time taken for waves propagates along the glass samples.

$$V = \frac{2X}{\Delta t} \quad (1)$$

Shear modulus (S), Young's modulus (E), bulk modulus (K), and Poisson's ratio ( $\sigma$ ) can be calculated from the following equations:

$$S = \mu \quad (2)$$

$$E = \frac{\mu (3\lambda + 2\mu)}{\lambda + \mu} \quad (3)$$

$$K = \lambda + \frac{2}{3}\mu \quad (4)$$

$$\sigma = \frac{\lambda}{2(\lambda + \mu)} \quad (5)$$

The values of  $\lambda$  and  $\mu$  are obtained from the longitudinal and shear ultrasonic velocities.

#### Rockwell Hardness Test

FUTURE-TECH Rockwell Hardness Tester FR Series was used in this research project to test the hardness of glasses. Scales were used to determine the hardness of RHA glass. A 1/16-inch ball was selected as indenter with 60 kg, 100 kg, and 130 kg load to conduct the hardness test on the RHA glass.

## RESULTS AND DISCUSSIONS

### Chemical Composition of RHA

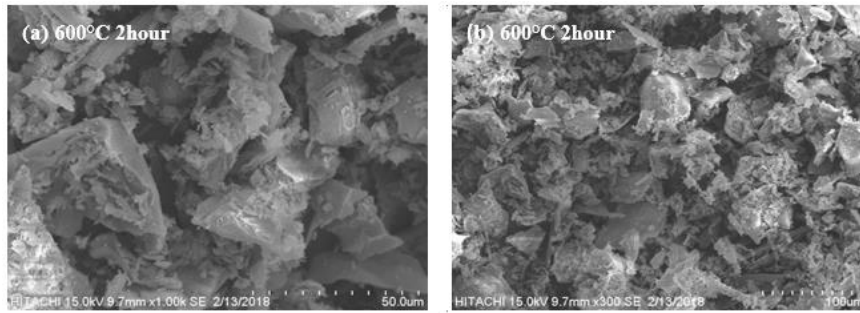
Table 2 shows the chemical composition of the RHA before sintering and SLS glass. The results illustrate that the main constituent of RHA is silica at 92.095 wt %, which is consistent with the findings of Mishra et al., who found that RHA contains approximately 92-97 wt % silica [12]. Table 2 also shows that the SLS glass contains 61.363 wt % silica, which is in accordance with values reported Bateni et al. [13]. It should also be noted that in addition to SiO<sub>2</sub>, RHA sample was found to contain other oxides such as CaO, Al<sub>2</sub>O<sub>3</sub>, TiO<sub>2</sub>, MgO and Na<sub>2</sub>O which were presumed to be impurities that tend to change the properties of material.

**Table 2.** The chemical composition of RHA and SLS glass

Elements	RHA (wt %)	SLS Glass (wt %)
SiO <sub>2</sub>	92.095	61.363
K <sub>2</sub> O	0.066	0.358
Al <sub>2</sub> O <sub>3</sub>	0.354	-
Fe <sub>2</sub> O <sub>3</sub>	0.031	0.847
CaO	0.008	37.432
TiO <sub>2</sub>	0.007	-
MgO	0.002	-
Na <sub>2</sub> O	0.003	-

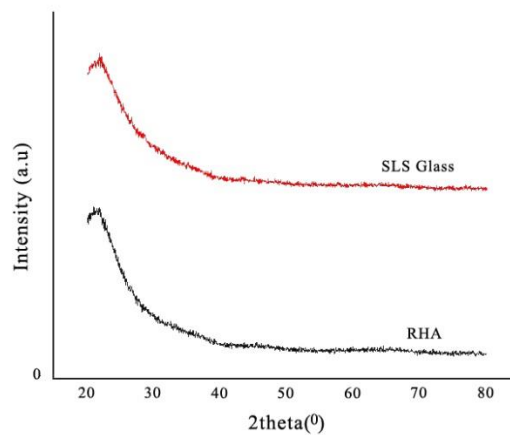
### Microstructural Characterization of RHA

Figure 4 depicts the SEM image of RHA sample incinerated with controlled temperature of 600 for two hours. By investigating the SEM image, RHA is in amorphous form as the silica particles were irregular and toothed in accordance to a study by Fernandes in 2017 [14]. RHA particles were gathered or assembled together due to the adhesion of silanol groups on the RHA particles surface with the occurrence of hydrogen [15]. Under higher magnification, certain irregular small debris was also observed and consist of less void spaces between the particles.



**Figure 4.** SEM micrograph of RHA at magnification: (a) X1000 and (b) X300

Validating through X-ray diffraction patterns as in Figure 5, this figure shows the amorphous structure of RH. A single diffuse band centred at  $21^\circ$ , which indicates the amorphous structure of the silica present in the RHA treated at  $600^\circ\text{C}$  for 2 hours and the SLS glass. This finding is consistent with the findings of Della et al. (2002), there was no diffuse peak appeared in the diffractogram [16]. This condition was also been studied by Liou (2004) and the results were in harmonise [17].



**Figure 5.** XRD analysis of RHA and SLS glass

#### Microstructural Characterization of SLS-RHA Glass

Figure 6 illustrates the SEM micrograph of SLS-RHA glass sample for 0, 5 and 10% wt. RHA. Pores and rough surface attributes are observed. SEM images show the increase in pores as RHA percentage increases. Figure 5(a) shows larger pores and less surface roughness compared to other samples. It is observed that the surface roughness increases as the RHA percentage increases. According to Lodins et al., sintering temperature affects the microstructure properties of glass as an incomplete glassy phase affects the roughness of the glass surface [18]. In Figure 5(b-c), open pores can be observed. It was found that the SLS-RHA glass with 10% wt. RHA addition is more porous and rougher which was in accordance with a research conducted by Wasanapiarnpong et al. [19]. Wasanapiarnpong et al. stated that with an increase addition of RHA produced glasses with various pore sizes and more porous. This is in good agreement with the result obtained for bulk density of the fabricated glass.

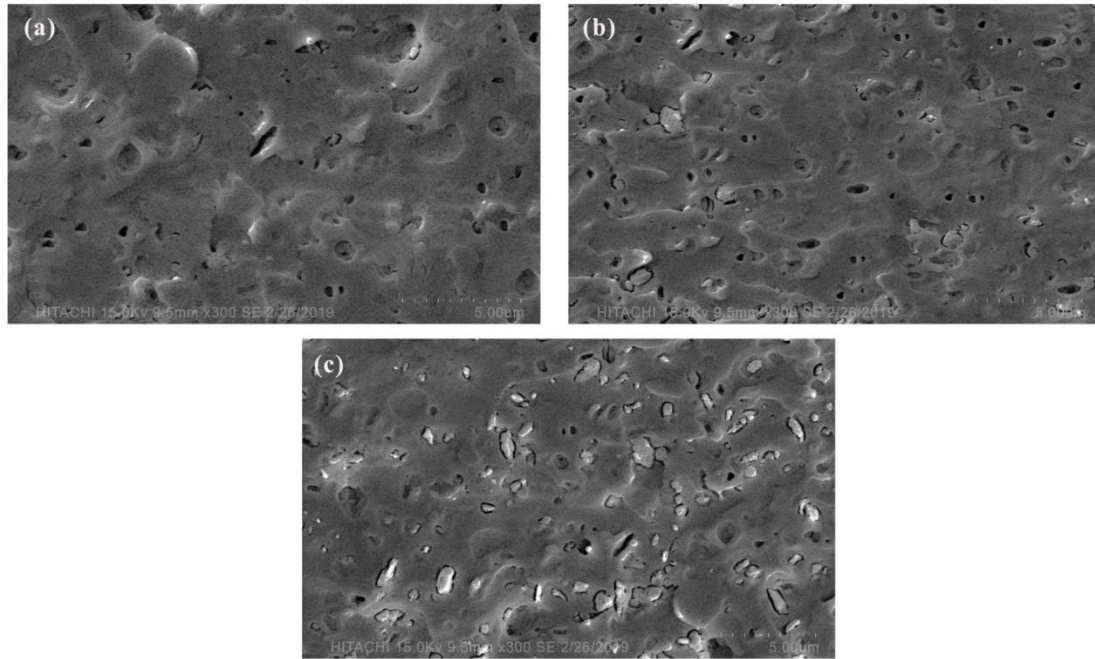


**Figure 6.** SEM images of SLS-RHA glass containing: (a) 0 % wt. RHA (b) 5% wt. RHA and (c) 10% wt. RHA sintered at 1400°C

### Ultrasonic Velocity Test

In evaluating the elastic properties of the SLS-RHA glass, the value of ultrasonic velocity was obtained by measuring the longitudinal time interval and shear time interval using MATEC Model MBS8000 DSP. Results of the longitudinal and shear time intervals for three different samples of RHA glass is showed in Table 3 and 4 respectively.

**Table 3.** Sample thickness, longitudinal time travel for SLS-RHA glass

Sample	Sample Thickness (m)	Density, $\rho$ ( $\text{gcm}^{-3}$ )	Longitudinal Time Interval $\Delta t$ (s)	Longitudinal velocity, $V_L$ ( $\text{ms}^{-1}$ )
1	0.01	2.520	$4.0161 \times 10^{-6}$	4980
2	0.01	2.553	$4.0866 \times 10^{-6}$	4894
3	0.01	2.598	$4.2310 \times 10^{-6}$	4727

**Table 4.** Sample thickness, shear time travel for RHA glass

Sample	Sample Thickness (m)	Density, $\rho$ ( $\text{gcm}^{-3}$ )	Shear Time Interval $\Delta t$ (s)	Shear velocity, $V_S$ ( $\text{ms}^{-1}$ )
1	0.01	2.520	$6.1406 \times 10^{-6}$	3257
2	0.01	2.553	$6.3532 \times 10^{-6}$	3148
3	0.01	2.598	$6.5020 \times 10^{-6}$	3076

From the obtained longitudinal and shear time intervals, the ultrasonic wave velocities which are longitudinal and shear velocities can be calculated using Eq. (1). The plotted graph for ultrasonic velocities against the percentage of RHA in the SLS-RHA glass is shown in Figure 7. It is observed, that as the percentage of RHA increases, the time of ultrasonic wave travels through SLS-RHA glass increase. Observation in Table 2 and 3 show that the calculated ultrasonic wave velocities ( $V_L$  and  $V_S$ ) decreased as the density of the SLS-RHA glass increased. Generally, the ultrasonic wave velocities for most of the samples will increased as the density of the materials increased. This is due to the increasing percentage of RHA, indirectly decreases the porosity as the interstitial cations ( $\text{Ca}^+$ ,  $\text{Na}^+$ ,  $\text{K}^+$ ) enter the vacant sites of the network in the SLS and increase the density of the SLS-RHA glass [20]. In addition, higher density of SLS-RHA glass density resulted an increase of the time interval of the wave in the ultrasonic test.

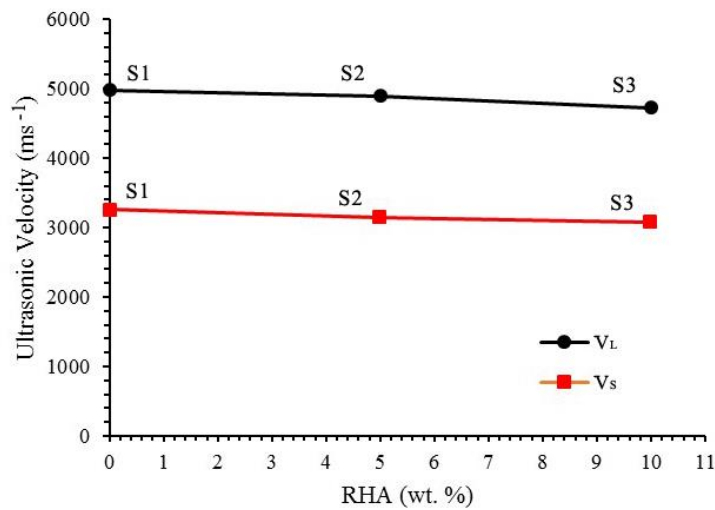


**Figure 7.** Ultrasonic velocity against the percentage of RHA in the RHA glass

The elastic properties of the SLS-RHA glass which are longitudinal modulus (L), shear modulus (S), Young's modulus (E), bulk modulus (K), and Poisson's ratio ( $\sigma$ ) of the RHA glass were obtained based on the value of the ultrasonic velocities. Elastic properties of the RHA glass samples are presented in Table 5.

**Table 5.** Elastic properties of SLS-RHA glass

Sample (%)	Longitudinal Modulus, L (GPa)	Shear modulus, S (GPa)	Young's modulus, E (GPa)	Bulk modulus, K (GPa)	Poisson's ratio, $\sigma$
0	62.498 <sup>[1]</sup>	26.732 <sup>[1]</sup>	140.778 <sup>[1]</sup>	26.854 <sup>[2]</sup>	0.1263 <sup>[3]</sup>
5	61.148 <sup>[2]</sup>	25.300 <sup>[2]</sup>	140.287 <sup>[2]</sup>	27.414 <sup>[1]</sup>	0.1471 <sup>[1]</sup>
10	58.051 <sup>[3]</sup>	24.582 <sup>[3]</sup>	131.517 <sup>[3]</sup>	28.275 <sup>[3]</sup>	0.1328 <sup>[2]</sup>

<sup>[1]</sup>: high properties, <sup>[2]</sup>: medium properties, <sup>[3]</sup>: low properties

Based on the elastic properties, the elastic moduli values decreased with the increasing percentage of RHA in the samples. The longitudinal modulus and shear modulus of RHA glass decreases with the increase of RHA content. The value of the longitudinal modulus decreases from 62.498 GPa to 58.051 GPa a 7.12% decrease for 0% to 10% rice husk glass series. The shear modulus of RHA glass also decreases from 26.732 GPa to 24.582 GPa with the increase of RHA content. The result for longitudinal modulus is higher compared to shear modulus which means the SLS-RHA glass could withstand a better longitudinal stress compared to shear stress. Due to its greater longitudinal stress value, the properties of SLS-RHA glass is easier to bend rather than to be elongated. Figure 8 shows the result of longitudinal modulus and shear modulus calculated from the ultrasonic wave velocities at different values of RHA weight percentage content. The elastic strain in an amorphous solid (glass) that produced from minor stress can be explained by two independent elastic constants which are longitudinal modulus and shear modulus [21].

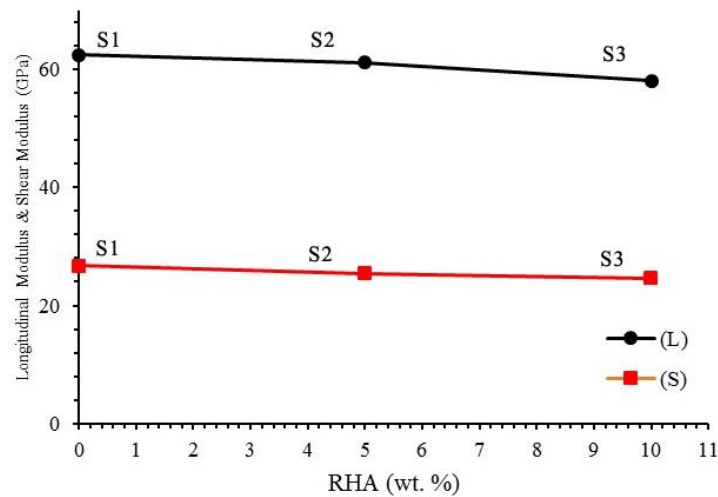


**Figure 8.** Longitudinal and shear modulus against the percentage of RHA in the SLS-RHA glass

The stiffness of materials based on the ratio of longitudinal stress over the strain is represented in Young's Modulus. The greater the Young's modulus the stiffer the materials becomes. In addition, the stiffness of materials are related to the strength of atoms bonding in the materials and the connectivity and dimensionality of the structure will influence the modulus of materials [22]. Based on Figure 8, Young's modulus of RHA glass decreases from 140.778 GPa to 131.517 GPa with the increase of the RHA contents. The decreases in value may due to the presence of non-bridging oxygen (NBO) in the RHA glass. Formation of NBOs will decrease the connectivity of the glass network and the structures of the glass become weakened [23]. When the connectivity of the glass network decreases, the glass becomes less stiff and less rigid caused by decreases in Young's modulus. By maintaining a lower Young's modulus in glass it helps to improve the impacting resistance of glass because of the slower the impact decelerated will develop a smaller stress in the glasses [24]. Hence, the SLS-RHA glass can endure the strains due to the smaller stress acting on the glass even though the glasses are less stiff.

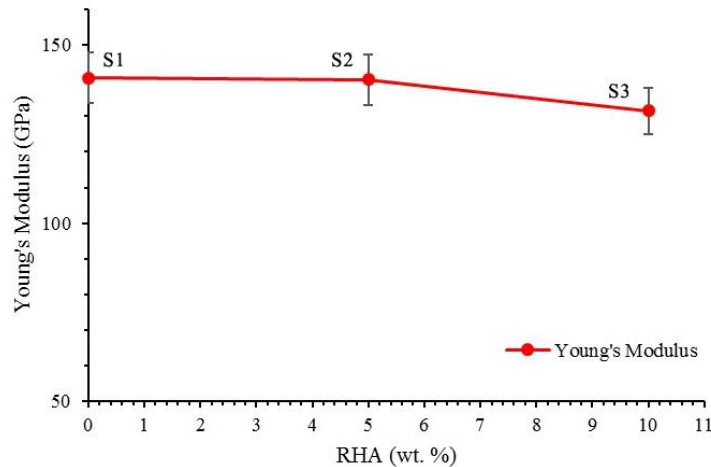


**Figure 8.** Young's modulus against the percentage of RHA in the SLS-RHA glass

### Rockwell Hardness Test

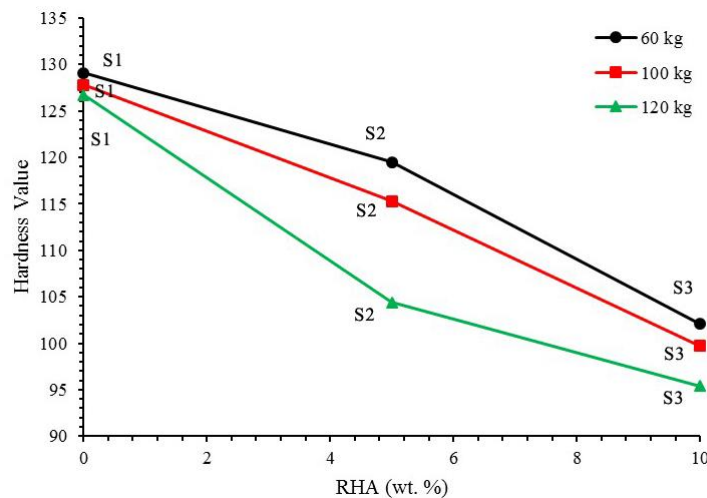
Elastic properties of materials can be studied using the ultrasonic wave velocity testing, however, the hardness of materials are not able to be obtained from the ultrasonic wave speed. Hence, Rockwell hardness can be carried out in order to investigate the hardness values for RHA glass as shown in Table 5. Hardness test used to study the resistance of glass to abrasion or scratch. Measurement of Rockwell hardness test is based on the permanent depth of penetration of an indenter with a load on the material. The high hydrostatic pressure in the glass will reduce free volume and become compacted [25].



**Table 5.** Elastic properties of RHA glass

Rockwell hardness test scales (kg)	Samples		
	0% RHA	5% RHA	10% RHA
60	129.1	119.5	102.1
100	127.8	115.3	99.7
120	126.7	104.4	95.4

The value of Rockwell hardness decreased with increasing percentage of RHA in the glass. The hardness value decreases because of the decreases in connectivity of the RHA glass structure. From results presented in Table 5, the Rockwell hardness value of rice husk hush ash glass decreases with increasing the load force or indenters force. The value of Rockwell hardness decreases from 129.1 when using 60kg indenters to 127.8 using 100kg indenters at 5% of RHA. The addition of RHA in the glass decreases the connectivity of glass structure due to increases formation of NBOs. Figure 9 shows the relationship between Rockwell hardness test scale, percentage of RHA and Rockwell hardness value.

**Figure 9.** Rockwell hardness value against the percentage of RHA in SLS-RHA glass

## CONCLUSIONS

A new combination of glass is produced using SLS waste with added RHA content. These glass were investigated to determine the effect of RHA addition on the physical properties of soda-lime-silica glass. SEM results indicate that with the addition of RHA, the surface of the glass became more porous and rougher. Results from ultrasonic velocity test showed that sample with 5% of RHA possessed a high and medium elastic properties which affect the mechanical properties of the glass. Sample with 5% RHA possesses properties which is easier to bend rather than elongate, less stiff, tough at a certain direction and has low rigidity. Sample with 0% and 10% of RHA showed medium and poor elastic properties, respectively. High hardness value of the RHA glass was achieved using the combinations of 60 to 120 Rockwell hardness test scale for 0 to 5% RHA. By considering the results from both test, sample with 0% to 5% of RHA was considered to be the best option to formulate the production of building glass and window panel.

## ACKNOWLEDGMENTS

The authors wish to acknowledge their gratitude to PIPPT grant 6387700 and Universiti Putra Malaysia.

## REFERENCES

- [1] J. Kanagaraj, T. Senthilvelan, R. C. Panda, S. Kavitha, "Eco-friendly waste management strategies for greener environment towards sustainable development in leather industry: A comprehensive review," *J. Clean. Prod.*, vol. 89, pp. 1–17, 2015, doi: 10.1016/j.jclepro.2014.11.013.
- [2] A. Abraham, A. K. Mathew, R. Sindhu, A. Pandey, P. Binod, "Potential of rice straw for bio-refining: An overview," *Bioresour. Technol.*, vol. 215, pp. 29–36, 2016, doi: 10.1016/j.biortech.2016.04.011.
- [3] R. Isaak, "The making of the ecopreneur," *Greener Manag. Int.*, no. 38, pp. 81–91, 2002, doi: 10.9774/GLEAF.3062.2002.su.00009.

- [4] C. S. Prasad, K. N. Maiti, R. Venugopal, "Effect of rice husk ash in whiteware compositions," *Ceram. Int.*, vol. 27, no. 6, pp. 629–635, 2001, doi: 10.1016/S0272-8842(01)00010-4.
- [5] M. S. Mohd Basri, F. Mustapha, N. Mazlan, M. R. Ishak, "Fire retardant performance of rice husk ash-based geopolymer coated mild steel - A factorial design and microstructure analysis," *Mater. Sci. Forum*, vol. 841, pp. 48–54, 2016, doi: 10.4028/www.scientific.net/MSF.841.48.
- [6] M. Kubo and M. Purevdorj, "The Future of Rice Production and Consumption," *J. Food Distrib. Res.*, vol. 35, no. 1, pp. 128–142, 2004.
- [7] S. Chandrasekhar, K. G. Satyanarayana, P. N. Pramada, P. Raghavan, T. N. Gupta, "Processing, properties and applications of reactive silica from rice husk - An overview," *J. Mater. Sci.*, vol. 38, no. 15, pp. 3159–3168, 2003, doi: 10.1023/A:1025157114800.
- [8] F. Andreola *et al.*, "Technological properties of glass-ceramic tiles obtained using rice husk ash as silica precursor," *Ceram. Int.*, vol. 39, no. 5, pp. 5427–5435, 2013, doi: 10.1016/j.ceramint.2012.12.050.
- [9] H. B. Dizaji *et al.*, "Generation of high quality biogenic silica by combustion of rice husk and rice straw combined with pre- and post-treatment strategies-A review," *Appl. Sci.*, vol. 9, no. 6, pp. 1–27, 2019, doi: 10.3390/app9061083.
- [10] V. Le Houérou, J. C. Sangleboeuf, S. Dériano, T. Rouxel, G. Duisit, "Surface damage of soda-lime-silica glasses: Indentation scratch behavior," *J. Non. Cryst. Solids*, vol. 316, no. 1, pp. 54–63, 2003, doi: 10.1016/S0022-3093(02)01937-3.
- [11] M. O. Prado, C. Fredericci, E. D. Zanotto, "Isothermal sintering with concurrent crystallization of polydispersed soda-lime-silica glass beads," *J. Non. Cryst. Solids*, vol. 331, no. 1–3, pp. 145–156, 2003, doi: 10.1016/j.jnoncrysol.2003.08.076.
- [12] P. Mishra, A. Chakraverty, H. D. Banerjee, "Production and purification of silicon by calcium reduction of rice-husk white ash," *J. Mater. Sci.*, vol. 20, no. 12, pp. 4387–4391, 1985, doi: 10.1007/BF00559326.
- [13] N. H. Bateni, M. N. Hamidon, K. A. Matori, "Effect of soda-lime-silica glass addition on the physical properties of ceramic obtained from white rice husk ash," *J. Ceram. Soc. Japan*, vol. 122, no. 1422, pp. 161–165, 2014, doi: 10.2109/jcersj2.122.161.
- [14] I. J. Fernandes *et al.*, "Characterization of silica produced from rice husk ash: Comparison of purification and processing methods," *Mater. Res.*, vol. 20, pp. 519–525, 2017, doi: 10.1590/1980-5373-mr-2016-1043.
- [15] M. Dominic, P. M. S. Begum, A. Jose, "Rice Husk Silica - Efficient BioFiller in High Density Polyethylene," no. January, 2014.
- [16] V. P. Della, I. Kühn, D. Hotza, "Rice husk ash as an alternate source for active silica production," *Mater. Lett.*, vol. 57, no. 4, pp. 818–821, 2002, doi: 10.1016/S0167-577X(02)00879-0.
- [17] T. H. Liou, "Preparation and characterization of nano-structured silica from rice husk," *Mater. Sci. Eng. A*, vol. 364, no. 1–2, pp. 313–323, 2004, doi: 10.1016/j.msea.2003.08.045.
- [18] E. Lodins *et al.*, "Characterization of glass-ceramics microstructure, chemical composition and mechanical properties," *IOP Conf. Ser. Mater. Sci. Eng.*, vol. 25, no. 1, 2011, doi: 10.1088/1757-899X/25/1/012015.
- [19] T. Wasanapiarnpong, B. Vorajesdarom, E. Rujirakamort, S. Nilpairach, C. Mongkolkachit, "Fabrication of silica glass from rice husk ash with spodumene additions," *IOP Conf. Ser. Mater. Sci. Eng.*, vol. 18, no. SYMPOSIUM 16, 2011, doi: 10.1088/1757-899X/18/22/222028.
- [20] J. Partyka and M. Leśniak, "Preparation of glass-ceramic glazes in the SiO<sub>2</sub>-Al<sub>2</sub>O<sub>3</sub>-CaO-MgO-K<sub>2</sub>O-Na<sub>2</sub>O-ZnO system by variable content of ZnO," *Ceram. Int.*, vol. 42, no. 7, pp. 8513–8524, 2016, doi: 10.1016/j.ceramint.2016.02.077.
- [21] D. Gross and T. Seelig, *Fracture Mechanics With an Introduction to Micromechanics Third Edition*. Springer International Publishing, 2018.
- [22] M. I. Mustaffar, M. H. Mahmud, M. A. Hassan, "Development of dense glass-ceramic from recycled soda-lime-silicate glass and fly ash for tiling," *AIP Conf. Proc.*, vol. 1901, 2017, doi: 10.1063/1.5010476.
- [23] E. M. A. Khalil, F. H. ElBatal, Y. M. Hamdy, H. M. Zidan, M. S. Aziz, A. M. Abdelghany, "Infrared absorption spectra of transition metals-doped soda lime silica glasses," *Phys. B Condens. Matter*, vol. 405, no. 5, pp. 1294–1300, 2010, doi: 10.1016/j.physb.2009.11.070.
- [24] K. A. Matori, M. H. M. Zaid, H. A. A. Sidek, M. K. Halimah, Z. A. Wahab, M. G. M. Sabri, "Influence of ZnO on the ultrasonic velocity and elastic moduli of soda lime silicate glasses," *Int. J. Phys. Sci.*, vol. 5, no. 14, pp. 2212–2216, 2010.
- [25] Y. B. Saddeek, "Ultrasonic study and physical properties of some borate glasses," *Mater. Chem. Phys.*, vol. 83, no. 2–3, pp. 222–228, 2004, doi: 10.1016/j.matchemphys.2003.09.051.